Open access • Journal Article • DOI:10.1016/0022-4073(91)90076-3

The continuum emission of an arc plasma — Source link

Arnold Theodoor Marie Wilbers, Gerrit Kroesen, CJ Timmermans, DC Daan Schram

Institutions: Eindhoven University of Technology

Published on: 01 Jan 1991 - Journal of Quantitative Spectroscopy & Radiative Transfer (Elsevier)

Topics: Spectroscopy, Electron density, Emission spectrum and Wavelength

The continuum emission of an arc plasma

J. Quant. Spectrosc. Radiat. Transfer Vol. 45, No. 1, pp. 1–10, 1991
Printed in Great Britain.

0022-4073/91 $3.00 + 0.00

THE CONTINUUM EMISSION OF AN ARC PLASMA

A. T. M. WILBERS, G. M. W. KROESEN, C. J. TIMMERMANS, and D. C. SCHRAM
Physics Department, Eindhoven University of Technology, P.O. Box 513, 5600 MB Eindhoven, The Netherlands

(Received 9 April 1990)

Abstract—We present free–bound Biberman factors (12,000, 13,500 and 14,500 K) for the wavelength range of 250–320 nm and 380–800 nm. These values were determined by measuring the absolute continuum intensity of a thermal argon plasma in a cascade arc (2 mm dia) for a pressure range of 2–6 × 10^5 Pa and a current range of 20–60 A. The continuum emission is corrected for free–free contributions. Two highly accurate experimental reference values of the free–bound factors were used to check the electron density. Agreement with experiments in the u.v. is good. Comparison with theoretical values also shows good agreement below 430 nm. Above this wavelength, theory predicts an edge structure which is not apparent in the available experimental values. The agreement between our results and recent experimental values (for which the electron density was obtained with two-wavelength interferometry) is good. The influence of non-equilibrium has been found to be negligible. We conclude that absolute continuum measurements are well suited to determine electron densities (visible spectroscopy) and electron temperatures (u.v. spectroscopy) by using the known free–bound Biberman factors. Prediction of the absolute intensity as a function of wavelength is possible within 10%.

INTRODUCTION

Continuum light sources that cover a large spectral range are applied in several analytical techniques. Depending on the nature of the technique, the range of interest may cover the u.v., visible or i.r. part of the spectrum. The cascade arc is such a continuum light source, which emits a relatively high intensity from the u.v. to the i.r.[1–5] It is important to be able to predict the radiated power per unit wavelength. Because line radiation makes no significant contribution to the total intensity for our experimental conditions, we will consider only the continuum intensity.

Continuum radiation originates from interaction of electrons with ionized or neutral atoms in a plasma. When the electrons recombine with the ions, the interaction is called free–bound. On the other hand, when the electrons remain free, the interaction is called free–free. For simple systems such as hydrogen, these interactions are well described by theory. With more complex systems such as rare gases, the standard theory is not sufficient. Biberman[6] introduced a correction which accounts for the deviation from the hydrogen-like structure. These so called Biberman factors have been calculated for argon by Schlüter.[7] Hofsaess[8–10] improved these calculations and extended the wavelength, temperature and atom ranges.

Experimental values of the Biberman factors are measured by various authors. The data for argon are given among others by the authors of Refs. 11–22. Some results for fluorine in an SF_6 plasma are also available.[23,24] However, the differences between theory and experiments are substantial. Hofsaess[9] calculated the free–free and free–bound Biberman factors for various elements for temperatures in the range of 3000–30,000 K and wavelengths ranging from 30 nm up to 1.8 μm. He predicts sharp edges in the free–bound Biberman factors corresponding to radiative recombination. However, in the experimental data, the edges of $4p$ (460 nm) and $3d$ (740 nm) are not apparent.[18,19,21] Also, for F and S, the edges in the visible wavelength regime have not been confirmed.[23,24]

In this work, we will determine the free–bound Biberman factors from 250 to 320 nm and from 280 to 800 nm by measuring the absolute emission of an argon arc in the pressure range 2–6 × 10^5 Pa.

THE CONTINUUM INTENSITY: THEORY

The continuum emissivity of the arc plasma is governed by the following expressions:[25]

$$\epsilon = \epsilon_{fb} + \epsilon_{ff}^{ei} + \epsilon_{ff}^{ea}, \tag{1}$$

where

$$\epsilon_{ff}^{ei} = \sum_z \frac{C_1}{\lambda^2} \frac{n_e n_z}{\sqrt{T_e}} z^2 \exp\left(-\frac{hc}{\lambda k T_e}\right) \xi_{ff}(\lambda, T_e, z), \tag{2}$$

$$\epsilon_{ff}^{ea} = \frac{C_2}{\lambda^2} n_e n_a \sqrt{T^3} Q(T_e) \left[\left(1 + \frac{hc}{\lambda k T_e}\right)^2 + 1\right] \exp\left(-\frac{hc}{\lambda k T_e}\right), \tag{3}$$

and

$$\epsilon_{fb} = \sum_z \frac{C_1}{\lambda^2} \frac{n_e n_z}{\sqrt{T_e}} z^2 \left[1 - \exp\left(-\frac{hc}{\lambda k T_e}\right)\right] \frac{g_{z,1}}{U_z} \xi_{fb}(\lambda, T_e, z). \tag{4}$$

In these expressions, the symbols have the following meanings: ϵ_{ff}^{ei} = free–free radiation caused by electron–ion interaction, ϵ_{ff}^{ea} = free–free radiation caused by electron–neutral interaction, ϵ_{fb} = free–bound radiation, λ = wavelength of the radiation, C_1 = electron–ion continuum constant (1.63×10^{-43} Wm^4 K$^{0.5}$ sr^{-1}), C_2 = electron–neutral continuum constant (1.026×10^{-34} Wm^4 K$^{1.5}$ sr^{-1}), $Q(T_e)$ = cross section for electron–neutral interaction,[26] h = Planck constant (6.626×10^{-34} J/Hz), n_e = electron density, n_a = neutral density, n_z = density of the ground state of z-fold ionized ions ($z = 0, 1, 2, \ldots$), T_e = electron temperature, ξ_{ff} = Biberman factor for free–free radiation, ξ_{fb} = Biberman factor for free–bound radiation, U_z = partition function of the system z.[27]

The values of the constants C_1 and C_2 have been adopted from Cabannes and Chapelle.[25] In Fig. 1, the relative contributions of several of the radiation mechanisms to the total intensity are shown as a function of wavelength. Here LTE (Local Thermal Equilibrium) is assumed and Biberman factors according to Hofsaess have been used. The temperature and pressure are taken

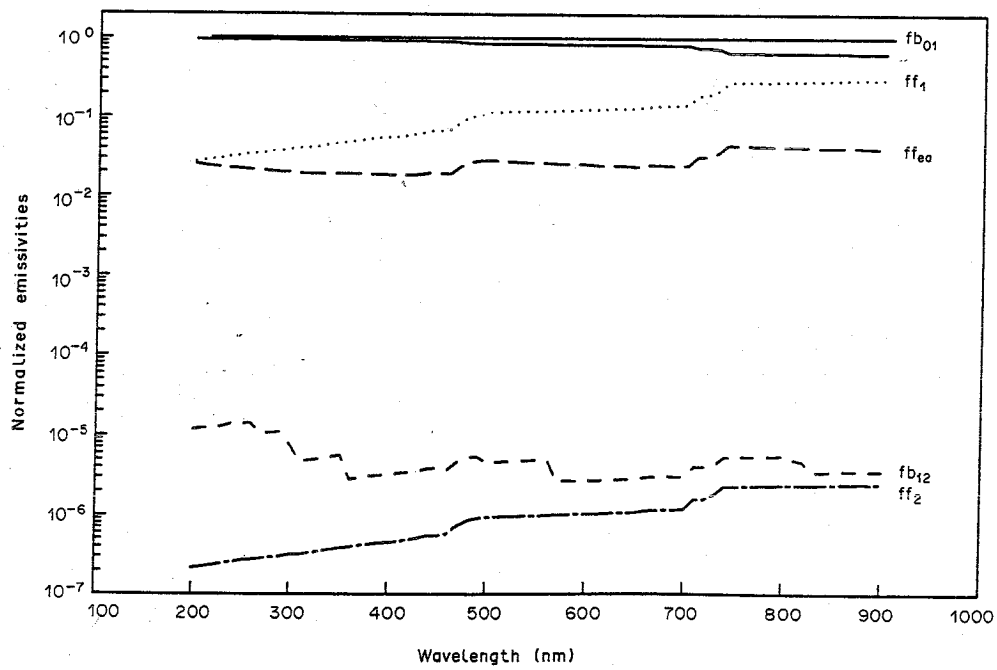

Fig. 1. The calculated emissivities normalized with respect to the total emissivity in the wavelength region covered for T_e of 13,500 K and a pressure of 4×10^5 Pa (LTE assumed). The symbols represent the following emissivities: fb_{01} = the free–bound of singly ionized atoms, fb_{12} = the free–bound of doubly ionized atoms, ff_1 = free–free of singly ionized atoms, ff_2 = free–free of doubly ionized atoms and ff_{ea} = the free–free of neutral atoms.

to be 13,500 K and 4×10^5 Pa, respectively. Figure 1 clearly shows that in the wavelength region covered the free–bound and free–free emissivity from interaction of electrons with singly-ionized ions is responsible for more than 95% of the total emissivity. Of these two, the free–bound contribution dominates below 600 nm (more than 90%). In the observed temperature and pressure regime the density of the singly ionized atoms is equal to n_e. It is clear then, from Eqs. (2) and (4) that emission from the argon plasma is only dependent on the square of n_e and on T_e (an inverse square root and an exponential factor) and depends only weakly on the neutral density. With increasing pressure and lower temperatures however, the free–free contribution arising from interaction with the neutral particles becomes more and more important. At 2×10^5 Pa and 13,500 K it is only 1.5% but at 4×10^5 Pa and 12,000 K it is already 6% (both values obtained at 500 nm). It is obvious that this contribution cannot be neglected when measuring at higher pressures and relative low temperatures. Also the importance of the electron–neutral contribution compared to electron–ion increases towards the u.v. At lower wavelengths (lower than 250 nm), the free–free electron–ion emissivity is even smaller than the electron–neutral contribution. Note that if the plasma is not in LTE, then the neutral density usually will be larger than the corresponding LTE value. This will enlarge the required corrections appreciably.

The emissivity is determined from intensity measurements. Accounting for the effect of absorption, the intensity emitted by the cascade arc is described by

$$I = S[1 - \exp(-\kappa l)] = S[1 - \exp(-\epsilon l/S)], \tag{5}$$

where the source function S is given by the Planck formula

$$S_\lambda = \frac{2hc^2}{\lambda^5}\left[\exp\left(\frac{hc}{\lambda k T_e}\right) - 1\right]^{-1}. \tag{6}$$

Here, κ is the absorption, ϵ the total emission and l the length of the discharge.

Although the excited levels are assumed to be in Saha equilibrium with the ions, the plasma will not be fully in LTE: the ground state density will deviate from the Saha value (partial LTE). We will parameterize this deviation with an overpopulation factor b of the ground level of the neutral argon system. This factor b is defined as

$$b = n_a/n_{a,S}, \tag{7}$$

where $n_{a,S}$ is the neutral density in Saha equilibrium. In our plasma which is ionizing, this factor will be larger than 1. If the plasma would be recombining, b could be smaller than 1. The validity of this concept has been shown by Rosado et al[28] and Nick et al[29] for electron densities larger than 6×10^{22} m^{-3}. Timmermans et al[30,31] have measured b for the conditions of 1×10^5 Pa and 5 mm arc diameter. In the temperature range from 9000 to 15,500 K, his values vary from 5 to 1.3, decreasing with increasing temperature.

From the measurements, we obtain an absolute value for the intensity I_{meas}. Using Eq. (5), we can calculate the absolute total emissivity ϵ_{meas}. Using the Saha equation, we can express the densities of the heavy particles in terms of n_e and T_e. Furthermore, quasi neutrality and Dalton's law link the various densities with each other and the measured total pressure.

The neutral density appears only in ϵ_{ff}^{ea}. If this contribution is smaller than a few percent (compare, e.g., the 2% calculated ϵ_{ff}^{ea} for 4×10^5 Pa and 13,500 K at LTE), then the measured absolute continuum intensity depends mainly on n_e (n_e^2) and on $T_e[T_e^{-1/2} \cdot \exp(-hc/\lambda k T_e)]$ in the observed temperature and pressure regime. If LTE independent methods are used to determine these two parameters, one can deduce the Biberman factors without specifying whether or not the plasma is fully in LTE. If the contribution of ϵ_{ff}^{ea} becomes larger (higher p, lower T), then the non-equilibrium neutral density should be calculated to apply the required corrections.

With the assumption of LTE (or PLTE and a b factor), two measured parameters are enough to characterize the plasma completely. Generally, the first parameter is the absolute pressure. The second parameter can be either n_e or T_e. The Biberman factors may then be determined from the measured absolute continuum intensity. How experimental or theoretical errors in the determination of n_e or T_e affect the calculated Biberman factors will be discussed in the following paragraphs.

From interferometry, we obtain n_e. The electron temperature can now be calculated either in LTE or in PLTE with a specified b factor. If non-equilibrium exists, the temperature will be slightly different. Because the u.v. part of the spectrum depends heavily on T_e [the influence of the exponent in Eq. (4) is strong in the u.v. in our n_e, T_e range], non-equilibrium will have a finite effect there. In the visible part of the spectrum, the influence of the temperature is weak and non-equilibrium effects will therefore also be weak. The relative effects of the PLTE and LTE neutral densities have already been mentioned.

The electron temperature can be determined from emission and absorption experiments; n_e may also be obtained but usually only one parameter is determined. Assuming LTE ($b = 1$), n_e can be calculated; if non-equilibrium exists, this n_e-value will be slightly too large. In the observed T_e and n_e regime, small errors in T_e will result in large errors in n_e. Therefore, a small change in T_e due to non-equilibrium will result in a significant change in n_e. The errors in the calculations of the Biberman factors from absolute intensities are even larger because the emissivity depends on the square of n_e. This error is the same over the entire wavelength region. A specification of the b factor is then necessary.

In this work, we will use the following procedure to obtain an electron density from the absolute continuum measurements. Three Biberman factors will be used at different wavelengths to calculate three values of the electron density; we will employ a theoretical Biberman factor at 400 nm (in this wavelength range theoretical and experimental values of the Biberman factor are in agreement within 5%) and two experimental values of the Biberman factor determined by Timmermans et al[32,33] at 468.8 nm and Rosado et al[34] at 700 nm. The experimental values were obtained from absolute continuum measurements together with accurate independent determinations of the electron density and electron temperature using the source function method and two-wavelength interferometry. The three values of the electron density thus obtained appear to be the same within 3%. Using this electron density, we may then calculate the Biberman factors for other wavelengths. The calculations will first be carried out with the assumption of LTE ($b = 1$). The influence of a $b \neq 1$ will be investigated at the end of our paper.

From the absolute line intensities of optically-thick lines (i.e., some lines above 700 nm), the electron temperature can be calculated. This temperature will be compared with the electron temperature calculated from the experimentally obtained electron density according to the procedure described above.

EXPERIMENTAL STUDIES

The cascade arc consists of three major sections: a cathode section, an anode section and a plate section between. The plate section, which holds five copper plates stacked into a cascade, gives the cascade arc its name. The whole system has a cylindrical geometry, with the plasma channel located on the symmetry axis. All sections are water-cooled. The sections and the plates are electrically insulated from one another by PVC-spacers. Boron-nitride disks protect the vacuum seals from damage caused by radiation emitted in the plasma channel. The cathode section contains three cathodes with sharply pointed thoriated tungsten tips. To allow for optical alignment, the cathode tips as well as the anode spot are not in the line of sight of the arc when it is observed end-on. The anode section holds the conical anode insert. The arc is operated in argon. A small flow, which replaces the arc volume about two times per second, is used to prevent gradual contamination of the arc plasma by cathode and wall material. The arc is ignited at reduced pressure (10^4 Pa) using a high-voltage power supply. Within 1 sec after ignition, the arc is pressurized to 1.5×10^5 Pa. In our case, each of the cathodes is fed by a separate power supply. Because of the negative voltage–current behavior of an igniting arc, series resistors (in our system 3 Ω) have to be included in the electrical setup.

OPTICAL SYSTEM

Two basically identical optical systems are used, one in the visible range and the other in the u.v. range. We will only discuss the setup used in the visible. With one lens (quartz) and two diaphragms, a small plasma volume (i.e., a cylinder of 0.5 mm dia) is selected. When a mirror is

rotated, a similar surface can be selected on the tungsten-strip lamp. Two additional lenses (quartz) increase the entrance angle to the optimum required value of the 1-m Jarrel Ash monochromator, which has an entrance angle of 0.1 rad and 50-micron slits. This setup was used in the visible wavelength region from 380 to 800 nm with a S20 photomultiplier (EMI 9698 QB). The lower wavelength region (115–320 nm) is measured in vacuum with LiF windows and lenses, in combination with a Seya–Namioka 0.5 m McPherson monochromator (entrance angle = 0.05 rad, slits = 100 micron in width) and a Solar Blind Photo multiplier (Hamamatsu R976) with an MgF_2 window. With this setup, the contribution of stray-light cannot be neglected below 180 nm. Because of the extreme intensity difference between the calibration lamp and the arc (2–5 orders of magnitude, depending on the wavelength region), a gray filter is used when the cascade arc is studied in the visible wavelength region. The current pulses which the photons induce in the photomultipliers are counted after being amplified, discriminated with respect to pulse height and converted to TTL pulses (photon counting). The signal treatment takes place as near as possible to the anode of the photomultiplier in order to eliminate noise. In this manner, we cover three orders of magnitude in intensity without losing linearity even though we have a low-intensity calibration lamp and a high-intensity cascade arc. The TTL pulses are fed into an interface card mounted in a personal computer. The absolute calibration is performed with the tungsten-ribbon lamp (Philips type W2 KGV 22i, No. 109, VSL 82 P 01) operated at a true temperature of 2667 K. The calibration of the lamp was performed at 655 nm at the Van Swinden laboratory VSL[35] (calibration report No. 661120096). The tables of De Vos[36] give the intensity of the lamp for the wavelength region covered.

RESULTS AND INTERPRETATION

Our measurements cover the wavelength regions of 250–320 and 380–800 nm. Extension to 115 nm (LiF window limit) is one of our future options.

Line radiation is present primarily in the wavelength region from 380 to 800 nm. From 250 to 320 nm, no significant line radiation could be detected. In Figs. 2 and 3, the measured spectra from 250 to 320 nm and 380 to 800 nm of the arc plasma are given for 4×10^5 Pa and 40 A. Figure 3 clearly shows the observed line radiation superimposed on strong continuum radiation.

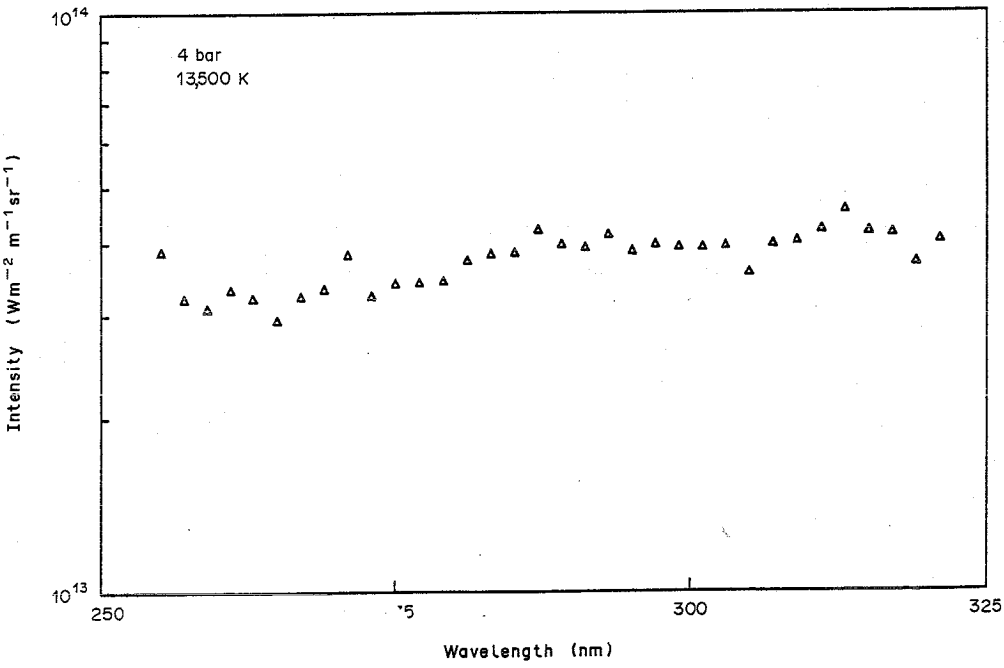

Fig. 2. The measured absolute intensities of a cascade arc between 250 and 320 nm for 4×10^5 Pa and 40 A.

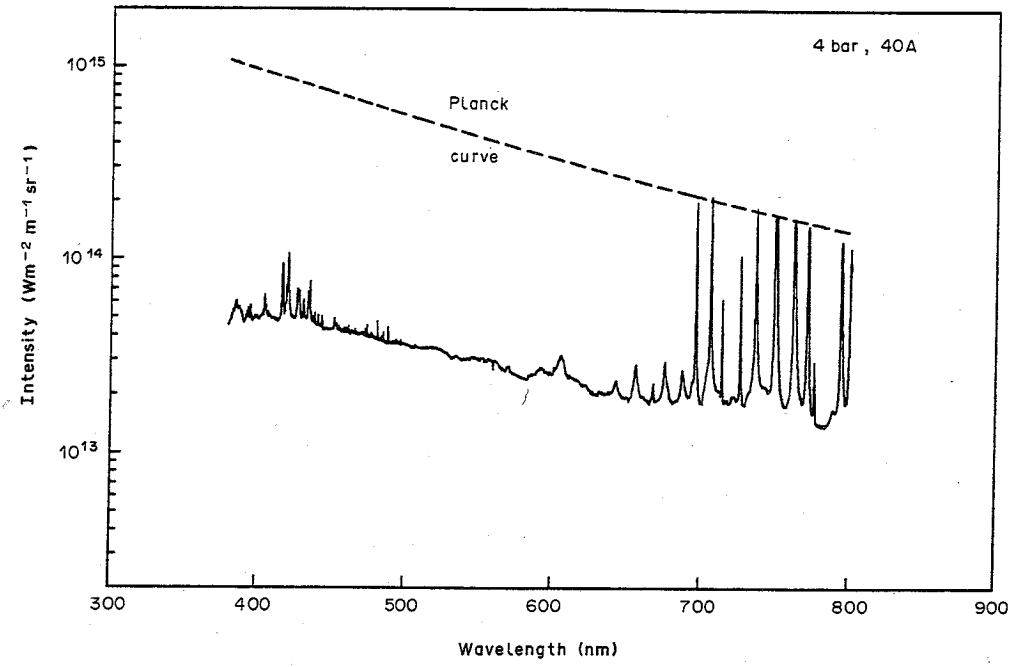

Fig. 3. The measured absolute intensities of a cascade arc between 380 and 800 nm for 4×10^5 Pa and 40 A, showing the observed line spectrum superimposed on the continuum.

From these absolute intensities, we have calculated the free–bound factors. For this purpose, 40 positions on the wavelength axis were selected in the region from 380 to 800 nm on the assumption that the continuum is sufficiently free of lines. In the low wavelength range (250–320 nm), all measurements could be used.

Both of the electron densities calculated from our measurements using the experimentally determined Biberman factors are in excellent agreement (within 3%) with the value calculated for the 400 nm determination of Hofsaess. The value at 400 nm has been used because the experimental results of several authors are in agreement with that of Hofsaess at this wavelength. The temperature used with Fig. 3 at the appropriate Planck limit was determined from the strongest observed lines above 700 nm, as may be seen in Fig. 3. This temperature is approx. 5% higher than the LTE value, which is an expected result with the measured b values at 1.013×10^5 Pa. The effect of this relatively higher temperature is negligible in calculating the electron density. The value of n_e appears to be equal to the n_e calculated from the absolute continuum. This result represents the fourth experimental verification of the electron density measurement.

In Fig. 4, calculated and measured free–bound Biberman factors, as obtained by various authors, are shown.

The differences between the various measured values can be explained in part by the methods for the determination of the plasma parameters n_e and T_e. Meiners,[16] Schnehage[19,20] and Zangers[22] used two-wavelength interferometry to determine n_e and then calculated T_e assuming LTE. Berge[11] determine these parameters with the help of the Rankine–Hugoniot equations and statistical thermodynamics from their shock-wave experiments. Erhardt,[12] Gall,[13] Schulz-Guide,[18] and Wende[21] used line intensities (uncertainties of 10–25% in the transition probabilities) of neutral and ionized argon to determine T_e. With the assumption of LTE, these authors calculated n_e and introduced errors of approx. 25% in the calculated free–bound factors. Goldbach[15] used line widths of neutral argon to determine n_e and line intensities for T_e. Morris[17] used several techniques and averaged the results. The variations in the free–bound factors of Schulz-Gulde are within his claimed accuracy. The values of Schulz–Gulde and Schnehage are the same, except for a constant difference of about 10% which is probably due to a difference in n_e of 5%. The values of Morris and Berge show a significantly higher level, whereas those of Gall only fit the values of Hofsaess for his lowest wavelength.

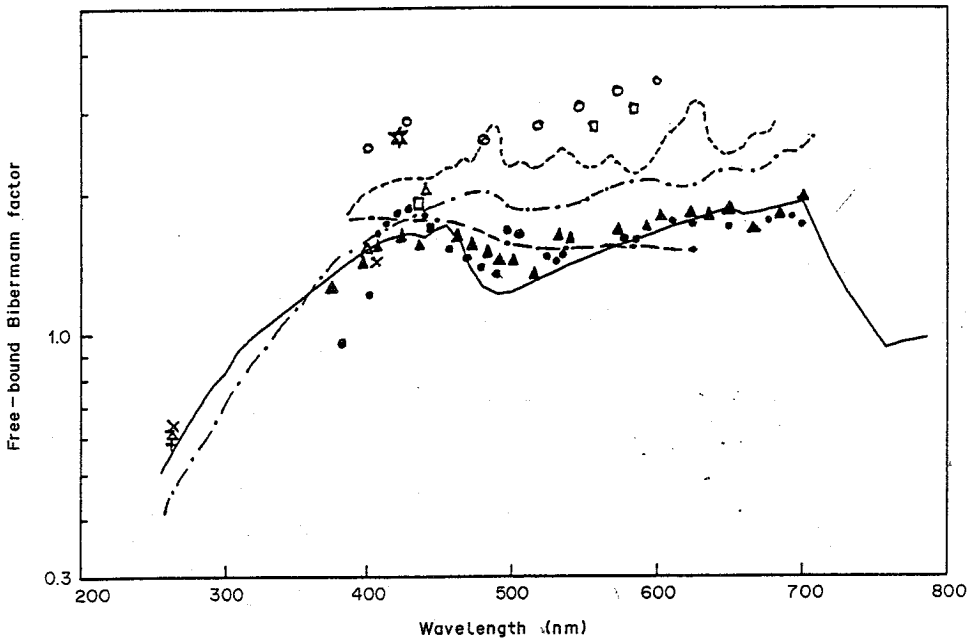

Fig. 4. The free–bound Bibermann factors. Measurements: (○) Berge; (●) Erhardt; (□) Gall; (×) Goldbach (1 atm); (+) Goldbach (5 atm); (△) Goldbach (30 atm); (■) Meiners (*) Morris; (▲) Schulz-Gulde; (–·–) Schnehage; (——) Wende; (—·—) Zangers; calculations by Hofsaess (—).

Determination of the electron density from two-wavelength interferometry is, in our opinion, the preferred method. The accuracy is very high and the LTE electron temperature calculated from this density is at most 500 K lower than the actual electron temperature.

From our measured free–bound emission, the free–bound Biberman factor is calculated by using the previously specified procedure. The accuracy of the absolute value of our Biberman factors is mainly due to the uncertainty in the plasma length in the present experiment. The uncertainty in this parameter is 10%. Then, the calculated electron density will also be accurate within 5%. Therefore, our Biberman factors, experimentally obtained, will have an accuracy of 10% (dependency of the square of n_e). The relative uncertainty over the entire wavelength range will be significantly smaller; in the visible part where $hc/\lambda kT_e < 1$ approx. 5% (calibration) and in the u.v. part somewhat larger due to the increased influence of the electron temperature. The effect of the uncertainty in the free–free Biberman factor of Hofsaess, which is needed to calculate the contribution of the free–free emissivity to the total emission, is small since the free–bound emissivity accounts for more than 90% of the total emission in this wavelength region (see Fig. 1). The free–free electron-neutral emission has been taken into account in our case, but again care has been taken that the contribution is small and consequently errors have little effect on the results. In Fig. 5, the result is shown for all plasma temperatures obtained in the measurements (12,000, 13,500 and 14,500 K), each averaged over the used pressures, together with the reference values of Timmermans et al[31,32] and Rosado et al.[33]

The pressure dependence of the Biberman factor is not noticeable within the error bars in the observed pressure range. According to theory and most experiments, there should not be any pressure dependence. Only Goldbach et al,[14,15] Gall et al[13] and Morris et al[17] detect pressure dependence. However, in Goldbach et al,[14] Gall et al and Morris et al the neutral contribution to the total emissivity is totally neglected. This contribution becomes increasingly important, 5% at approx. 4×10^5 Pa, and 15% at 30×10^5 Pa (12,000 K, LTE). Also, Goldbach et al[14] use line widths of the H_β line to determine n_e. They use a mixture of 98% argon and 2% hydrogen. However, because the ionization degree is very low (1%), the contribution of the hydrogen continuum could be substantial. Goldbach et al[15] include the neutral contribution according to LTE, but state that the effect is still too weak to account for the observed pressure dependence of the Biberman factor. However, non-equilibrium effects would increase the contribution to the continuum radiation by

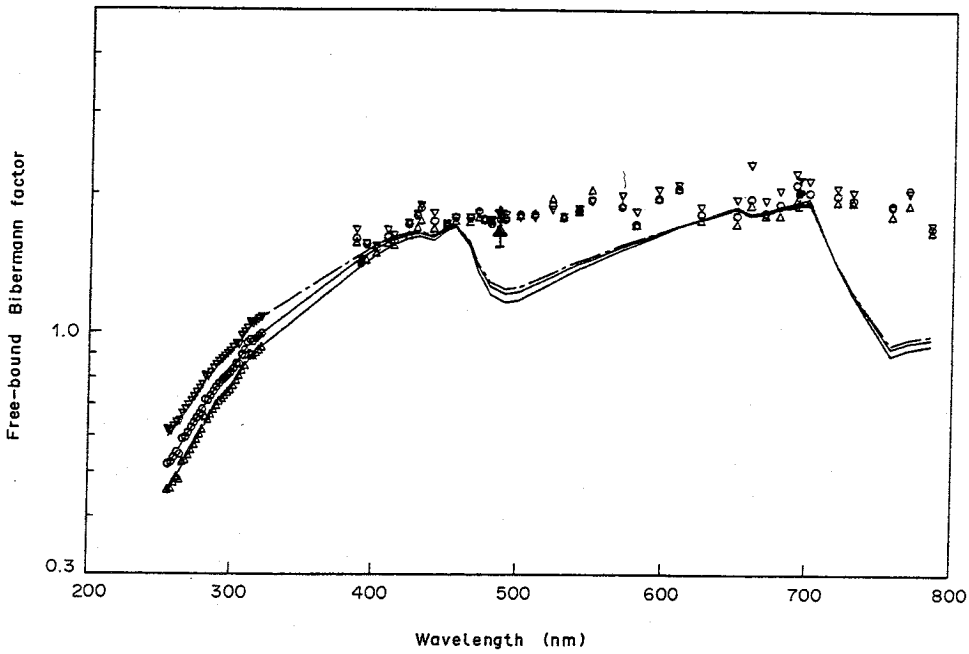

Fig. 5. The free–bound Bibermann factors according to our measurements, our reference values and those of Hofsaess: (△) 12,000 K; (○) 13,000 K; (▽) 14,500; (▲) Timmermans;[31,32] (●) Rosado;[33] calculations by Hofsaess (—).

a realistic b factor of 5 or more. It would be better to decrease the influence of the neutrals by carefully choosing the discharge parameters as has been done in our measurements.

We now discuss the wavelength dependence of our measurements. At 500 nm (Fig. 5) the deviation from Hofsaess amounts to almost 30%. Above 700 nm the deviation rises to values of more than 100%. However, in this region also line emission may contribute to the measured emission. At 785 nm, where a significant line free spectrum is found, the deviation is approx. 80%. Zangers and Meiners state that many weak lines, which are strongly broadened contribute to the measured emission and should therefore not be neglected. However, our measurements, which are not corrected for possible contributions from broadened lines, agree well with those of Zangers and Meiners. A possible explanation could be that the influence of the lines at higher pressures decreases. Park[37] calculated the contribution of the line emission to the free–bound and free–free Biberman factor and presents a total Biberman factor. This model fits the experimental results rather well except for the $4p$ edge at 460 nm.

To check the sensitivity of the calculations of the Biberman factors for non-equilibrium, we varied the b factor from 0.3 to 10 and repeated the calculations for each b factor. In Fig. 6 the free–bound Biberman factor at two wavelengths is shown as a function of the overpopulation together with the electron density and the electron temperature, normalized with respect to their values at b equals 1.

In the expected region of 1–5 of the overpopulation, the variation is only 5% at 12,000 K and smaller at higher temperatures. Therefore, the LTE-procedure is justified.

CONCLUSIONS

We have measured the absolute continuum emission in the wavelength ranges from 250 to 320 nm and 380 to 800 nm to determine free–bound Biberman factors of argon, using three known values of the Biberman factors to calculate the electron density. Our studies did not show a measurable pressure dependence.

We conclude from our measurements that using these Biberman factors and the absolute continuum intensity, accurate calculations of electron densities and electron temperatures of argon plasmas in an atmospheric arc are possible. In the visible wavelength range, the electron density

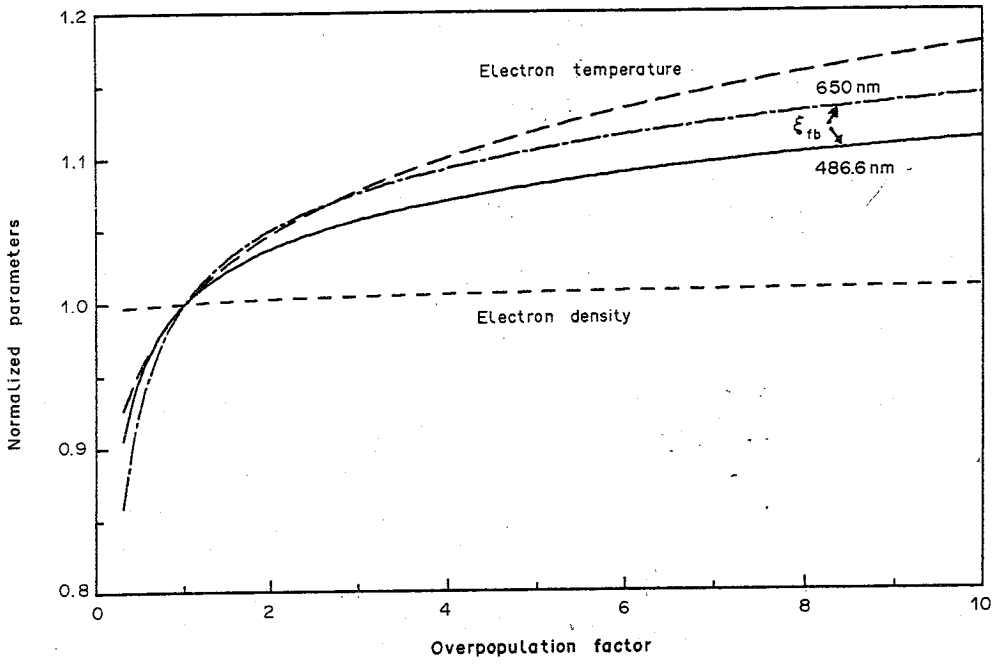

Fig. 6. The free–bound Bibermann factor at 486 and 650 nm as functions of b. The electron densities and temperatures are shown as functions of b normalized with respect to their values for $b = 1$.

can be determined with high accuracy. Below 430 nm, the accuracy is 5% and both experimental Biberman factors or the Biberman factors of Hofsaess may be used. Behringer and Thoma[38] showed that the lower wavelength limit may be extended to 140 nm for temperatures below 16,900 K. Clearly, the argon arc will serve as a high-intensity, secondary radiation standard in this wavelength range. The Biberman factor in the range from 430 to 800 nm may be taken from the available experimental results presented in Fig. 5 for the pressure range $1–6 \times 10^5$ Pa. The wavelength range may then be extended for use of the cascade arc as a high-intensity radiation standard from 430 to 800 nm. The accuracies in this wavelength range are determined by the accuracies and the ranges of the available experimental values of the Biberman factors. At high pressures, the effects of non-equilibrium should be taken into account.

The Biberman factors of argon calculated by Hofsaess agree well with our measurements over the entire observed wavelength range, except for the edges corresponding to the $4p$ and $3d$ series. In all of the experimental studies, including ours, these edges were not observable or else were much weaker than predicted by Hofsaess. A possible explanation could be a smoothing due to microfield distribution.

Acknowledgements—This work is part of the research program of the "Stichting voor Fundamenteel Onderzoek der Materie (FOM)," which is financially supported by the "Nederlandse organisatie voor wetenschappelijk onderzoek (NWO)." The authors thank R. de Rooij, R. van Haren and M. Dirkx who took part in the measurements in the course of their studies at our University. We acknowledge the skillful technical assistance of M. J. F. van de Sande and L. A. Bisschops. The authors thank A. B. M. Hüsken for assistance with electronics.

REFERENCES

1. J. Z. Klose, J. M. Bridges, and W. R. Ott, "Radiometric Standards in the Vacuum Ultraviolet," NBS special publication 250-3, Washington, DC (1987).
2. G. M. W. Kroesen, C. J. Timmermans, and D. C. Schram, *Proc. 8th Int. Symp. Plasma Chemistry*, p. 1097, Tokyo, Japan (1987).
3. G. M. W. Kroesen, Ph.D. Thesis, Eindhoven University of Technology, Eindhoven, The Netherlands (1987).
4. M. Haverlag, G. M. W. Kroesen, and F. J. de Hoog, *Proc. 9th Int. Symp. Plasma Chemistry*, p. 441, Pugnochiuso, Italy (1989).

5. A. T. M. Wilbers, G. M. W. Kroesen, C. J. Timmermans, and D. C. Schram, *Proc. 9th Int. Symp. Plasma Chemistry*, p. 302, Pugnochiuso, Italy (1989).
6. L. M. Biberman and G. E. Norman, *Opt. Spectrosc.* **8,** 230 (1960).
7. D. Schlüter, *Z. Phys.* **210,** 80 (1968).
8. D. Hofsaess, *JQSRT* **19,** 339 (1978).
9. D. Hofsaess, private communication (1982).
10. D. Hofsaess, *Atom. Data Nucl. Data Tables* **24,** 295 (1979).
11. O. E. Berge, A. Böhm, and L. Rehder, *Z. Naturf.* **20a,** 120 (1964).
12. K. Erhardt, I. Meyer, and P. Stritzke, *Z. Naturf.* **32a,** 21 (1977).
13. D. Gall and M. Riemann, *Beitr. Plasmaphys.* **10,** 1 (1970).
14. C. Goldbach, G. Nollez, and P. Plomdeur, *JQSRT* **12,** 1089 (1972).
15. C. Goldbach, G. Nollez, and P. Plomdeur, *J. Phys. B: Atom. Molec. Phys.* **10,** 1181 (1977).
16. D. Meiners and C. O. Weiss, *JQSRT* **16,** 273 (1976).
17. J. C. Morris and R. U. Krey, *JQSRT* **9,** 1633 (1969).
18. E. Schulz-Gulde, *Z. Phys.* **230,** 449 (1970).
19. S. E. Schnehage, M.Sc. Thesis, Institute für Plasma Physik, Hannover, B.R.D. (1980).
20. S. E. Schnehage, M. Kock, and E. Schulz-Gulde, *J. Phys. B: Atom. Molec. Phys.* **15,** 1131 (1982).
21. B. Wende, *Z. Phys.* **198,** 1 (1967).
22. J. Zangers and D. Meiners, *JQSRT* **42,** 25 (1989).
23. A. Gleizes, M. Razafinimanana, M. Sabsabi, and S. Vacquié, *JQSRT* **42,** 593 (1989).
24. H. Kafrouni and S. Vacquié, *JQSRT* **32,** 219 (1984).
25. F. Cabannes and J. C. Chapelle, in *Reactions Under Plasma Conditions*, M. Venugopalan ed., Wiley–Interscience, New York, NY (1971).
26. R. S. Devoto, *Phys. Fluids* **16,** 616 (1973).
27. H. W. Drawin and P. Felenbok, *Data for Plasmas in Local Thermodynamic Equilibrium*, Gautheir-Villars, Paris (1965).
28. R. J. Rosado, D. C. Schram, and J. Leclair, *Proc. XIIth Int. Conf. on Plasmas and Ionized Gases*, p. 573, Berlin (1977).
29. K. P. Nick, J. Richter, and V. Helbig, *JQSRT* **32,** 1 (1984).
30. C. J. Timmermans, Ph.D. Thesis, Eindhoven University of Technology, Eindhove, The Netherlands (1984).
31. C. J. Timmermans, G. M. W. Kroesen, P. M. Vallinga, and D. C. Schram, *Z. Naturf.* **40a,** 810 (1985).
32. C. J. Timmermans, private communication (1989).
33. C. J. Timmermans, G. A. J. Hermkens, and J. Batenburg, *Proc. 6th European Sectional Conf. on Atomic and Molecular Physics of Ionized Gases*, p. 179, London, U.K. (1982).
34. R. J. Rosado, D. C. Schram, and J. Leclair, *J. de Phys.* **C7,** 285 (1979).
35. Van Swinden Laboratory, P.O. Box 654 2600 AR Delft, The Netherlands (1985).
36. J. C. de Vos, *Physica* **20,** 690 (1954).
37. C. Park, *JQSRT* **28,** 29 (1982).
38. K. Behringer and P. Thoma, *JQSRT* **16,** 671 (1976).